Title
Loss of CpSRP54 function leads to a truncated light-harvesting antenna size in Chlamydomonas reinhardtii

Journal
Biochimica et Biophysica Acta (BBA) - Bioenergetics, 1858(1)

ISSN
0005-2728

Authors
Jeong, Jooyeon
Baek, Kwangryul
Kirst, Henning
et al.

Publication Date
2017

DOI
10.1016/j.bbabio.2016.10.007

Peer reviewed

Biochimica et Biophysica Acta 1858 (2017) 45–55

Contents lists available at ScienceDirect

Biochimica et Biophysica Acta

journal homepage: www.elsevier.com/locate/bbabio

Loss of CpSRP54 function leads to a truncated light-harvesting antenna size in *Chlamydomonas reinhardtii*

Jooyeon Jeong [a], Kwangryul Baek [a], Henning Kirst [b], Anastasios Melis [b,*], EonSeon Jin [a,*]

[a] Department of Life Science and Research Institute for Natural Sciences, Hanyang University, Seoul 133-791, Republic of Korea
[b] Department of Plant and Microbial Biology, University of California, Berkeley, CA 94720-3102, USA

ARTICLE INFO

Article history:
Received 28 May 2016
Received in revised form 14 October 2016
Accepted 14 October 2016
Available online 17 October 2016

Keywords:
Chlorophyll antenna size
CpSRP54
LHC assembly
Photosynthesis
Productivity
TLA technology

ABSTRACT

The *Chlamydomonas reinhardtii truncated light-harvesting antenna* 4 (*tla4*) DNA transposon mutant has a pale green phenotype, a lower chlorophyll (Chl) per cell and a higher Chl *a*/*b* ratio in comparison with the wild type. It required a higher light intensity for the saturation of photosynthesis and displayed a greater per chlorophyll light-saturated rate of oxygen evolution than the wild type. The Chl antenna size of the photosystems in the *tla4* mutant was only about 65% of that measured in the wild type. Molecular genetic analysis revealed that a single plasmid DNA insertion disrupted two genes on chromosome 11 of the mutant. A complementation study identified the "chloroplast signal recognition particle 54" gene (*CpSRP54*), as the lesion causing the *tla4* phenotype. Disruption of this gene resulted in partial failure to assemble and, therefore, lower levels of light-harvesting Chl-binding proteins in the *C. reinhardtii* thylakoids. A comparative *in silico* 3-D structure-modeling analysis revealed that the M-domain of the CpSRP54 of *C. reinhardtii* possesses a more extended finger loop structure, due to different amino acid composition, as compared to that of the *Arabidopsis* CpSRP54. The work demonstrated that *CpSRP54* deletion in microalgae can serve to generate *tla* mutants with a markedly smaller photosystem Chl antenna size, improved solar energy conversion efficiency, and photosynthetic productivity in high-density cultures under bright sunlight conditions.

1. Introduction

Photosynthesis depends on the absorption and conversion of sunlight energy by the photosystems, localized in the chloroplast thylakoid membranes. Photosynthetic organisms have developed an extensive light-harvesting system, composed of highly organized photosynthetic pigments within thylakoid membrane-embedded proteins that absorb and channel the light energy towards the photochemical reaction centers. Plants and green algae have developed large arrays of such chlorophyll-carotenoid (Chl-Car) light-harvesting complexes associated with the reaction centers of photosystem-I (PSI) and photosystem-II (PSII). The light-harvesting Chl-Car-binding proteins (LHCPs) comprise up to 50% of the thylakoid membrane proteins [1] and, therefore, are the most abundant membrane proteins on earth [2–5]. The *Lhca* and *Lhcb* gene subfamilies encode LHCA and LHCB proteins for the light-harvesting complex I (LHCI) associated with PSI and light-harvesting complex II (LHCII), associated with PSII, respectively [6].

Nuclear-encoded LHC proteins are synthesized in the cytosol and immediately imported into chloroplasts prior to insertion and assembly in the developing thylakoid membranes. While in transit in the chloroplast stroma, they are guided toward the portion of the thylakoid membrane where assembly of new photosystems takes place by the so-called signal recognition particle (SRP)–dependent pathway [7]. LHCPs and some PSII-core and PSI-core proteins use the chloroplast equivalent of the SRP pathway (CpSRP) for transmembrane assembly [2–5]. In a temporal sequence of events, the chloroplast stromal proteins CpSRP43 and CpSRP54 bind to imported target proteins; the receptor protein CpFtsY recognizes the CpSRP43–CpSRP54–target complex and guides it to the integral thylakoid membrane protein ALBINO3 (ALB3) [8,9]. ALB3 facilitates integration of the target protein into the thylakoid membrane [7]. The function of the CpSRP pathway in green microalgae slightly differs from that in higher plants [10–12]. This is evident from previous work on CpSRP43 and CpFTSY, recently identified and studied in *Chlamydomonas reinhardtii* [10,11]. The respective knockout mutants lacking these proteins exhibited lower total chlorophyll content and LHCP deficiency but normally functional photosystems, which are typical features of a **T**runcated **L**ight-harvesting **A**ntenna (TLA) phenotype.

Abbreviations: CCU, carbon capture and utilization; Chl, chlorophyll; Chl-Car, chlorophyll-carotenoid; CpSRP54, chloroplast signal recognition particle 54; LHCI, light-harvesting complex I; LHCII, light-harvesting complex II; LHCPs, Chl-Car-binding light-harvesting proteins; PSI, photosystem-I; PSII, photosystem-II; TLA, truncated light-harvesting antenna.

* Corresponding authors.
E-mail addresses: melis@berkeley.edu (A. Melis), esjin@hanyang.ac.kr (E. Jin).

http://dx.doi.org/10.1016/j.bbabio.2016.10.007
0005-2728/

It has been reported that high-density cultures of microalgae with a truncated light-harvesting antenna are photosynthetically more productive under bright sunlight and high-density growth conditions than cultures with fully pigmented cells. This improvement is due to mitigation of over-absorption and wasteful dissipation of excess energy by the outermost layer of cells in the culture, permitting greater transmittance of sunlight and culture productivity [13–17]. Thus, identification of genes that confer a permanent truncated light-harvesting antenna size phenotype in higher plants and green algae is of considerable interest, because such genes could be used to improve solar energy-to-biomass conversion efficiencies [17–19]. Recent results from *in vivo* analysis of *Chlamydomonas reinhardtii* TLA mutants with defects in LHCP transport and integration into thylakoids via the CpSRP pathway have demonstrated a drastic lowering in the cellular content of Chl and light-harvesting complexes in these mutants [10,11]. The mutants with the loss of function of CpFTSY and CpSRP43 were referred to as *tla2* and *tla3*, respectively. However, the role of the CpSRP54 protein in the assembly of the LHC in *Chlamydomonas*, and the role this protein plays as a tool in the generation of TLA-mutants, have not been investigated.

In this work, we isolated a new truncated light-harvesting antenna (TLA)-type strain from a library of *C. reinhardtii* strains generated by DNA insertional mutagenesis. We present a molecular, genetic, and physiological analysis of the newly identified mutant, termed *tla4*, which had a stably truncated light-harvesting Chl antenna. The corresponding *TLA4* gene was cloned and found to encode a homolog of the plant CpSRP54 protein. Functional analyses revealed a smaller light-harvesting Chl antenna size in the *tla4-CpSRP54* mutant in *C. reinhardtii* and a greater per Chl productivity of this strain relative to the wild type.

2. Materials and methods

2.1. Cell growth conditions

Chlamydomonas reinhardtii wild-type strains CC-4349 cw15 mt- (provided by the laboratory of Dr. Jae-Hyeok Lee) and DNA insertional transformants were maintained at 25 °C. Cells were cultivated photoheterotrophically in Tris-acetate phosphate (TAP) medium, or photoautotrophically in high-salt (HS) and Tris-bicarbonate phosphate (TBP) medium [20] under continuous low or medium irradiance (70 or 350 μmol photons m^{-2} s^{-1}, respectively).

2.2. Mutagenesis and mutant selection

Mutants of *C. reinhardtii* CC-4349 were constructed by random DNA insertional mutagenesis by agitating cells with glass beads as described in [21]. A PCR product amplified from the plasmid pPEARL [22], which contained a paromomycin resistance gene, was introduced into the parental strain CC-4349. Specific primers (PAR_vector-F and PAR_vector-R) were used for PCR product amplification (Supplementary Table S1). Transformants were selected on TAP medium containing 1.5% agar with 50 μg/mL paromomycin and screened upon measurement of Chl fluorescence with a Walz Imaging PAM System (M-series) equipped with a CCD camera. Among the initially screened transformants, mutants with altered pigment compositions were further selected on the basis of their Chl *a*/*b* ratios.

2.3. Cell counts and pigment determination

Samples were harvested from the exponential growth phase of cultures grown in HS medium. Cell number in cultures was estimated by counting with a Neubauer Bright Line hemacytometer and an Olympus CH30 microscope. The Chl content of cells was spectrophotometrically determined in 100% (v/v) methanol extracts according to the method of [23]. Total carotenoid was measured as previously described in [24].

2.4. Measurements of photosynthetic activity

Cells were grown in HS medium under 70 μmol photons m^{-2} s^{-1} and aliquots were removed from the culture during the exponential growth phase. Oxygen evolution was measured at 25 °C with a Clark-type oxygen electrode illuminated with red LED light (660 nm). A 1 mL aliquot of cell suspension containing 2 μM Chl was transferred to the oxygen electrode chamber. To ensure that oxygen evolution was not limited by carbon supply available to the cells, 50 μL of 0.5 M $NaHCO_3$ (pH 7.4) was added to the cell suspension before measurements. After registration of dark respiration, the rate of oxygen exchange was measured at increasing light intensities (20, 40, 60, 80, 100, 300, 500, 700, 900, 1200 and 1500 μmol photons m^{-2} s^{-1}). Baseline registration and the rate of oxygen evolution at each light intensity step were recorded for 2 min.

2.5. Isolation of thylakoid membranes

Cells were grown photoautotrophically at 250 μmol photons m^{-2} s^{-1} under continuous bubbling with air in the TBP growth medium. Cells were harvested by centrifugation at 1000*g* for 3 min at 4 °C. Samples were resuspended with ice-cold sonication buffer containing 50 mM Tricine (pH 7.8), 10 mM NaCl, 5 mM $MgCl_2$, 0.2% polyvinylpyrrolidone 40, 0.2% sodium ascorbate, 1 mM aminocaproic acid, 1 mM aminobenzamidine, and 100 mM phenylmethylsulfonyl fluoride. Cells were broken by sonication in a Branson 250 Cell Disrupter operated at 4 °C three times for 30 s each time (pulse mode, 50% duty cycle, output power of 5) with 30 s cooling intervals on ice. Cell debris and starch grains were removed by centrifugation at 3000*g* for 4 min at 4 °C. Thylakoid membranes were collected by centrifugation of the first supernatant at 75,000*g* for 30 min at 4 °C. The pellet of thylakoid membrane was resuspended in a buffer containing 50 mM Tricine (pH 7.8), 10 mM NaCl, and 5 mM $MgCl_2$ for spectrophotometric measurements.

2.6. Spectrophotometric and kinetic analyses

Spectrophotometric measurements of the amplitude of the light-minus-dark absorbance difference signal at 700 nm (P700) for PSI and 320 nm (Q_A) for PSII were used to estimate the concentration of the photosystems in thylakoid membranes [25,26]. The kinetics of P700 photooxidation and Q_A photoreduction of DCMU-poisoned thylakoid were measured under weak green actinic excitation and the corresponding rate constants were used to estimate the functional light-harvesting Chl antenna size of PSI and PSII, respectively [26].

2.7. Cell growth analysis

To measure the biomass accumulation properties of the *tla4* culture relative to that of the wild type, we carried out comparative growth analyses with each of the two cultures grown upon bubbling with 6% CO_2, under 450 μmol photons m^{-2} s^{-1}, i.e., a light intensity greater than that required to saturate photosynthesis in the wild type. Cultures were bubbled with airflow velocity of 40 mL/min at 25 °C. The *C. reinhardtii* cells were grown in 200 mL HS media in a bubble column photobioreactor with 4 cm diameter and 50 cm height.

Rate of microalgal growth was measured during the exponential growth phase from the increase in cell number as a function of time. The growth rate (μ) was calculated from the following equation [27]:

$$\mu = \ln(N_2/N_1)/(t_2-t_1) \quad (1)$$

where N_1 and N_2 are the cell counts at times t_1 and t_2, respectively.

2.8. Isolation of nucleic acids

Cells harvested from the exponential growth phase were centrifuged at 2600*g* for 10 min. The pellet was resuspended in 750 μL of microprep buffer containing (final concentrations) 2.5× extraction buffer (0.35 M Sorbitol, 0.1 M Tris/HCl pH 7.5, and 5 mM EDTA), 2.5× nuclear lysis buffer (0.2 M Tris/HCl pH 7.5, 0.05 M EDTA, 2 M NaCl, and 2% (w/v) CTAB), and 5% *N*-lauroylsarcosine. Cells were lysed by incubation at 65 °C and extracted by mixing them with 750 μL of chloroform:isoamyl alcohol (24:1) followed by centrifugation at 13,000*g* for 5 min. The upper phase was transferred to another tube and mixed with 350 μL of ice-cold isopropanol to precipitate DNA, followed by centrifugation at 13,000*g* for 5 min. The DNA pellet was washed twice with 70% ethanol and resuspended in distilled water.

2.9. Southern blot analysis

Genomic DNA was digested by various restriction enzymes (*Nco*I, *Sma*I and *Pst*I; Takara), the digests were separated on a 0.6% agarose gel, transferred onto a positively charged nylon membrane (Hybond-N+; Amersham), and UV cross-linked. Probes were obtained by PCR amplification from the pPEARL plasmid and labeled with alkaline phosphatase using the Gene Images AlkPhos Direct Labeling and Detection System kit (Amersham). The manufacturer's protocol was used for labeling, hybridization, washing, and signal detection.

2.10. Analysis of genomic DNA regions flanking the plasmid insertion site

A Seegene DNA Walking SpeedUp kit was used. Primers are listed in Supplementary Table S1. The manufacturer's protocol was followed in all procedures. Nucleotide sequences of the resulting PCR products were analyzed using the JGI Comparative Plant Genomics Portal (http://phytozome.jgi.doe.gov/pz/portal.html#!info?alias=Org_Creinhardtii).

2.11. Complementation experiments

For complementation of the *tla4* mutant, the *CpSRP54* cDNA was cloned into the pChlamy3 plasmid (Life Sciences) and introduced into the genomic DNA of the *tla4* mutant by using the glass-bead transformation method [21]. The pChlamy3 plasmid contains a hygromycin resistance gene and Hsp70A and RbcS2 fusion (AR) promoters, which drive the expression of the *CpSRP54* gene. Complemented strains were selected on TAP medium containing 1.5% agar with 10 μg/mL hygromycin and screened to assess color appearance and the Chl *a*/*b* ratio.

2.12. SDS-PAGE and Western blot analysis

SDS-PAGE analysis was carried out according to [28]. Lanes were loaded on the basis of equal cell number (3×10^6 cells per lane). After protein separation, gels were stained with 0.1% (w/v) Coomassie Brilliant Blue R or blotted onto an ATTO P PVDF membrane in a semi-dry transfer system. Membranes were probed with polyclonal antibodies against LHC and PS core proteins. Anti-LHCA (1–2) and anti-LHCB (1–3, 5) from *A. thaliana* and LHCB4, LHCBM5, PsaC, PsbA, PsbD, PsbO, RbcL, and ATPβ from *C. reinhardtii* antibodies were purchased from Agrisera. *C. reinhardtii* anti-LHCA 3, 4 and 9 antibodies were kindly donated by Dr. Michael Hippler [29]. Anti-CrCpFTSY, anti-CrCpSRP43, and anti-CrCpSRP54 antibodies were generated by Dr. Henning Kirst [10,11]. Signals were visualized by using the Abfrontier west save up ECL Reagent and exposed to an X-ray film for signal detection. The National Institutes of Health ImageJ 1.48 software was used for deconvolution and quantification of protein bands.

2.13. Modeling of 3D structure

The folding structures of CpSRP54 from *Arabidopsis thaliana* and *Chlamydomonas reinhardtii* were modeled by using the Phyre web server version 2.0 in intensive mode [30]. The GenBank accession number of AtCpSRP54 used in this analysis is NP_196014. A putative chloroplast-targeting sequence predicted by ChloroP software (http://www.cbs.dtu.dk/services/ChloroP/) was removed from each query sequence (*A. thaliana*, amino acids 75–564; *C. reinhardtii*, amino acids 4–549). The predicted model was visualized by using PyMOL version 1.74 (Schrödinger, Inc.).

2.14. Data analysis and statistics

Data in all experiments are mean value ± SD from three biological replicates. Significant differences between wild type and *tla4* were determined by using Student *t*-test. The statistical significance was indicated as c, d if $p < 0.01$ and as a, b if $p < 0.001$.

3. Results

3.1. Chlamydomonas reinhardtii strains with a truncated light-harvesting antenna

A library of 9216 mutant strains was constructed by random DNA insertional mutagenesis of the *C. reinhardtii* strain CC-4349 (*cw15 mt-*). PCR products amplified from pPEARL [22] were introduced into wild-type cells [21]. Transformants were selected on media containing paromomycin, which was possible because the exogenous PCR fragment contained a paromomycin resistance cassette. TLA strains are predicted to have a low yield of Chl fluorescence and high Chl *a*/*b* ratio [10,11,16]. Based on these properties, colonies of transformants on agar were initially screened by Chl florescence and then, in a second screening step, by the Chl *a*/*b* ratio to identify putative *tla* mutants. The first screening step helped identify 83 putative TLA mutants with lower Chl fluorescence yield than the parental wild-type strain. Among them, two strains had a substantially higher Chl *a*/*b* ratio than the control, indicating that they were putative TLA-type mutants. One of these mutants, termed *tla4*, was grown on TAP-agar (heterotrophic) and HS-agar (autotrophic) media to further test for colony coloration and Chl fluorescence properties (Fig. 1). Visually, the *tla4* strain colony was pale green, whereas wild-type strain CC-4349 was dark green

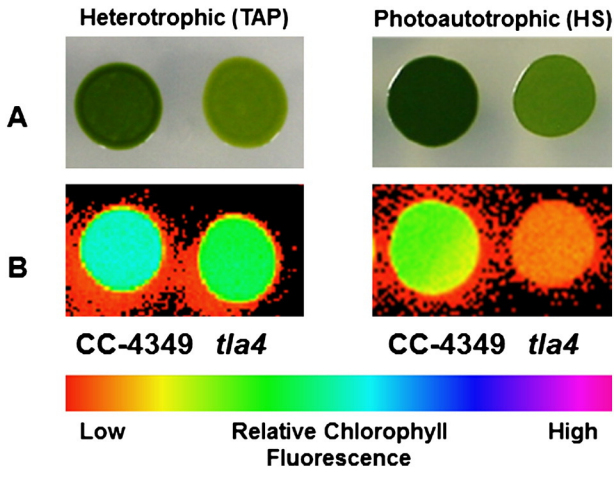

Fig. 1. Coloration (A) and false-color fluorescence imaging (B) of *C. reinhardtii* grown on agar heterotrophically (Tris-acetate phosphate medium; TAP) or autotrophically (high-salt medium; HS). Wild-type strain CC-4349 (parental strain of *tla4*) and the *tla4* mutant were grown under low light (100 μmol photons m^{-2} s^{-1}). Note the dark-green coloration of the wild-type strain and the pale-green color of the *tla4* mutant, which underlies the substantially lower yield of Chl fluorescence (red color).

(Fig. 1A). Thus, the *tla4* mutant showed visual coloration phenotype similar to that of previously isolated *tla1–tla3* mutants [10,11,16]. Furthermore, as shown in Fig. 1B, the wild-type strain displayed Chl fluorescence yields similar to each other with a relatively high Chl fluorescence emission, whereas the *tla4* mutant showed lower levels of Chl fluorescence emission. These preliminary results are consistent with a smaller Chl antenna size for the *tla4* mutant.

3.2. Lower pigment content and altered pigment composition in the tla4 mutant

The pigment content of wild type and *tla4* strains was measured upon growth in liquid cultures under low light (LL: 70 μmol photons m^{-2} s^{-1}) and medium light (ML: 350 μmol photons m^{-2} s^{-1}) conditions (Fig. 2). Regardless of the growth light condition, the *tla4* mutant had a lower Chl content per cell and a higher Chl *a*/*b* ratio than the wild type. The Chl *a*/*b* ratio of the recipient CC-4349 strain was 2.44 and 2.6 under low light and medium light conditions, respectively. By comparison with this wild type control, the *tla4* mutant had a significantly greater Chl *a*/*b* ratio, 3.33 (LL) and 3.69 (ML) (Fig. 2A). The higher Chl *a*/*b* ratio in *tla4* suggested absence of a portion of Chl *b* and potentially a smaller Chl antenna size in this mutant since Chl *b* is specifically associated with the periphery of the photosystems light-harvesting complexes.

The parental strain of the *tla4* mutant (CC-4349) contained 0.92 fmol Chl per cell under LL and 0.54 fmol Chl per cell under ML, whereas the respective values for the *tla4* mutant were 0.55 (LL) and 0.3 (ML). Accordingly, under both growth-irradiance conditions the total Chl content of the *tla4* mutant was down to about 57% of that in the recipient control strain (Fig. 2B). The total carotenoid content of the *tla4* mutant was also lower than that of the wild type strain (Fig. 2C).

3.3. Efficiency and productivity of photosynthesis in wild type and tla4 mutant

To investigate the functional properties of the photosynthetic apparatus in the wild type and *tla4* mutant, the light saturation curves of photosynthesis were measured from the rate of O_2 evolution as a function of incident light intensity on a per Chl basis (Fig. 3) and cell basis (Supplementary Fig. S1). Photosynthetic activity on a per Chl basis increased as a function of irradiance in the light intensity range of 0 to 200 μmol photons m^{-2} s^{-1}. Between 20 and 200 μmol photons m^{-2} s^{-1}, the increasing rate was linear for both strains (Fig. 3). From the linear regression slopes, the quantum yield of photosynthesis of each strain was determined [17]. The slope was 0.103 for *tla4* and 0.095 for the wild type. Each value was converted to relative units and normalized to the wild-type control, resulting in values of 108.6 for *tla4* and 100 for the wild type. These results demonstrate that the quantum yield of the photosynthetic apparatus is similar in wild type and *tla4* mutant, i.e., the *tla4* mutation did not adversely affect the quantum yield of photosynthesis in this strain (Table 1).

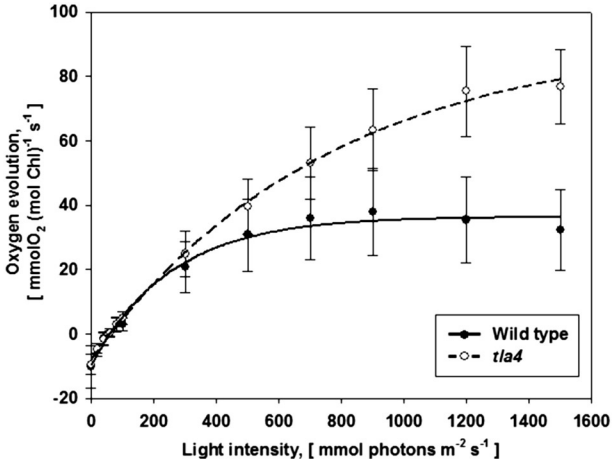

Fig. 3. Light-saturation curves of photosynthesis in wild-type *C. reinhardtii* and the *tla4* mutant (n = 4–10; values shown are means ± SD). Rates of oxygen evolution on a per Chl basis were measured as a function of incident light intensity. The initial slopes of both curves were similar, suggesting similar quantum yield of photosynthesis. Light-saturated photosynthetic rate (P_{max}) is about 84% higher in the *tla4* mutant than in the wild type, suggesting a greater photosynthetic capacity on a per Chl basis in *tla4* than in the wild type.

In the CC-4349 recipient strain, photosynthesis was fully saturated at about 350 μmol photons m^{-2} s^{-1} (Fig. 3 and Supplementary Fig. S1). However, the photosynthetic activity of the *tla4* mutant continued to increase beyond this light intensity and did not quite saturate even at 1500 μmol photons m^{-2} s^{-1}, a consequence of the substantially truncated antenna size in the *tla4* mutant. The maximum photosynthetic rate (P_{max}) on a Chl basis was 42.08 ± 2.13 mmol oxygen (mol Chl)$^{-1}$ s^{-1} for the wild type (Table 1) and 77.48 ± 6.28 mmol oxygen (mol Chl)$^{-1}$ s^{-1} for the *tla4* mutant (Table 1), i.e., about 80% greater. When measured on a cell basis, the maximal rate of O_2 evolution of *tla4* was about the same as that in the wild type, 30.72 ± 2.56 and 30.66 ± 4.05 fmol oxygen (10^6 cells)$^{-1}$ s^{-1} for *tla4* and the wild type, respectively (Table 1). Respiration rates were, within experimental error,

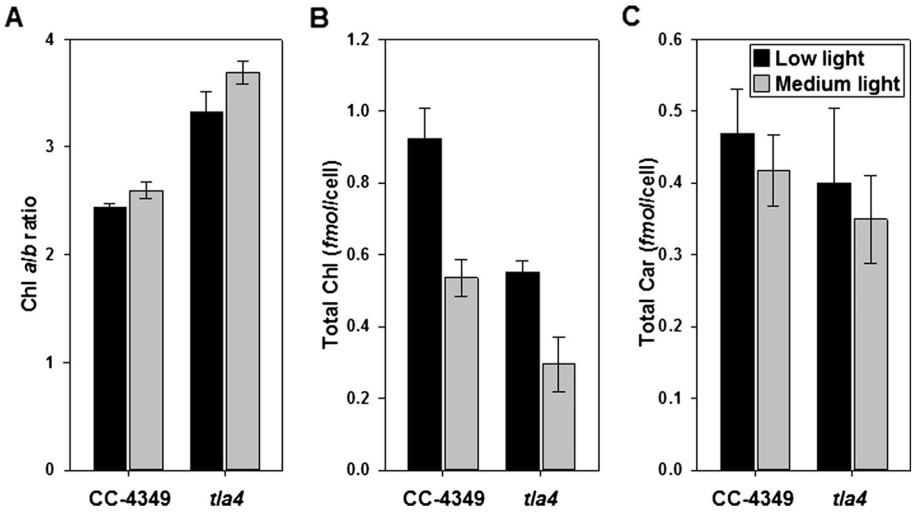

Fig. 2. Chlorophyll (Chl) and carotenoid (Car) pigment contents and the Chl *a*/*b* ratio of wild-type strain CC-4349 (parental strain of *tla4*) and the *tla4* mutant (n = 4–6; values shown are means ± SD). Black bars: low light (70 μmol photons m^{-2} s^{-1}) grown cells. Gray bars: medium light (350 μmol photons m^{-2} s^{-1}) grown cells.

Table 1
Photosynthetic and photochemical characteristics of wild type *C. reinhardtii* and the *tla4* mutant. The size of the photosystems I and II Chl antennae and reaction center concentrations were measured spectrophotometrically ([26]; n = 3; values shown are means ± SD). Cells were grown photoautotrophically at 250 μmol photons m^{-2} s^{-1} under continuous bubbling with air in the TBP growth medium.

Parameter measured	Wild type	*tla4*
Respiration [mmol oxygen (mol Chl)$^{-1}$ s^{-1}]	11.14 ± 1.83	9.49 ± 1.59
Respiration [fmol oxygen (10^6 cells)$^{-1}$ s^{-1}]	6.43 ± 2.64	3.81 ± 1.27
P_{max} [mmol oxygen (mol Chl)$^{-1}$ s^{-1}]	42.08 ± 2.13	77.48 ± 6.28
P_{max} [fmol oxygen (10^6 cells)$^{-1}$ s^{-1}]	30.66 ± 4.05	30.72 ± 2.56
Quantum yield, relative units	100 ± 5.29	108.63 ± 12.41
Photosynthesis [mmol oxygen (mol Chl)$^{-1}$ s^{-1}]	53.22 ± 3.13	86.97 ± 5.76
Total Chl/total Q_A (PSII)	458 ± 81	325 ± 37
Total Chl/total P700 (PSI)	500 ± 19	289 ± 15
PSII/PSI ratio	1.09 ± 0.20	0.89 ± 0.11
Proportion $PSII_\alpha$ [%]	0.29 ± 0.05	–
Proportion $PSII_\beta$ [%]	0.71 ± 0.04	1.00 ± 0.00
Functional $PSII_\alpha$ Chl antenna size	247 ± 19	–
Functional $PSII_\beta$ Chl antenna size	189 ± 8	151 ± 12
Average PSII Chl antenna size	205 ± 11	151 ± 12
Functional PSI Chl antenna size	276 ± 9	154 ± 3

about the same in the two strains on a Chl basis, while *tla4* individual cells consumed lower amounts of oxygen compared to the control (6.43 ± 2.64 fmol oxygen (10^6 cells)$^{-1}$ s^{-1} for wild type and 3.81 ± 1.27 fmol oxygen (10^6 cells)$^{-1}$ s^{-1} for *tla4*).

3.4. Photosynthetic apparatus organization and chlorophyll antenna size of the photosystems in the wild type and tla4 mutant

To compare the photosynthetic apparatus organization of *tla4* and wild type, the absolute amount of photochemically active Q_A and P700 was measured by sensitive absorbance difference spectrophotometry [25,26]. This method is well-established in our lab, and has been used successfully to provide measurement of photosystem concentration and photosystem chlorophyll antenna size in diverse photosynthetic tissues [10–19,25,26,31,32]. Table 1 shows the amounts of functional Q_A (PSII) and P700 (PSI) that were measured from the light-induced absorbance changes at 320 and 700 nm, respectively. Ratios of total Chl, PSII, and PSI from isolated samples were estimated. Total Chl to PSII and total Chl to PSI were significantly greater in the wild type (458 ± 81 for PSII and 500 ± 19 for PSI) than in the *tla4* mutant (325 ± 37 for PSII and 289 ± 15 for PSI), strengthening the notion that there is less Chl relative to the photosystems, i.e., a TLA phenotype, in this mutant. Moreover, the PSII/PSI stoichiometric ratio was lowered to 0.89:1 in the *tla4* mutant, compared to 1.09:1 measured in the recipient control strain (Table 1).

The specific functional Chl antenna size of PSII and PSI was then determined by the use of the kinetic/spectrophotometric method [26]. In this method, functional Chl molecules are assigned to the PSI or PSII reaction center in direct proportion to the rates of weak green light absorption and utilization by the respective photosystem. PSI and PSII antenna sizes are measured from the kinetics of Q_A photoreduction and P700 photooxidation in isolated and DCMU-treated thylakoids, respectively [26]. Wild-type thylakoids exhibited biphasic Q_A photoreduction kinetics, indicating the existence of two populations of PSII reaction centers, $PSII_\alpha$ and $PSII_\beta$. However, in *tla4*, the Q_A photoreduction was slower and monophasic; thus, *tla4* possessed only a single type of uniform antenna PSII units. The average number of Chl molecules associated with PSII in the wild type was 205 ± 11 and in the *tla4* mutant 151 ± 12 (i.e., lower by about 27%; Table 1). In both the wild type and *tla4*, photo-oxidation of P700 occurred with monophasic exponential kinetics, showing the presence of a uniform in terms of antenna population of PSI units. The average functional PSI Chl antenna size in the *tla4* (154 ± 3) was also smaller than that of the wild type (276 ± 9) by about 44%.

The totality of the above results (Table 1) is consistent with a TLA-phenotype in the *tla4* mutant. There is, however, a qualitative difference between this work (*tla4*) and earlier findings (*tla2*, *tla3*). In the latter, a proportionally greater loss of Chl occurred in PSII, whereas in the *tla4* mutant in this work, proportionally more Chl was lost from the antenna of PSI, rather than of PSII. This is reflected in the compensation of the photosystem ratio [31], whereby the *tla2* and *tla3* mutants showed an accentuated PSII/PSI ratio (compensation for the proportionally smaller PSII antenna size; [10,11]), whereas the *tla4* mutant showed a suppressed PSII/PSI ratio (Table 1), consistent with a compensation for the proportionally smaller PSI antenna size in this mutant.

Cell growth rates as a function of time were measured from the cell duplication time during the exponential growth phase, according to standard procedure (please see Materials and methods) [27]. Growth curves of wild type and *tla4* mutant under saturating 450 μmol photons m^{-2} s^{-1} irradiance are shown in Supplementary Fig. S2, and growth rate measurements are summarized in Table 2. The wild type exhibited a growth rate of 0.097 ± 0.007 h^{-1}, whereas the *tla4* mutant showed a growth rate as 0.154 ± 0.005 h^{-1}, which is 1.59-fold greater than that of the wild type. Similarly, at the end of the growth phase, the wild type reached a cell density of 4.09×10^7 cells/mL, whereas that of the *tla4* culture had 4.7×10^7 cells/mL, which is 15% greater than that of the wild type (Supplementary Fig. S2). The greater stationary phase biomass accumulation in the *tla4* than wild type culture is attributed to less nitrogen required for the synthesis of LHC proteins and chlorophylls in this mutant. The extra available nitrogen was apparently invested toward attaining a greater cell density/biomass in the culture.

3.5. Molecular characterization of the tla4 mutant

To establish the connection between the observed phenotype and the gene affected by the exogenous DNA insertion, the number of insertion events was ascertained by Southern blot analysis. A DNA probe was designed from the exogenous *aphVIII* paromomycin resistance cassette (Fig. 4A). Southern blot analysis of wild type (WT) and *tla4* genomic DNA showed results consistent with a single plasmid insertion into the genomic DNA of the *tla4* mutant (Fig. 4A). Chromosome walking was used to identify the site of plasmid insertion into the genomic DNA. The sequences of the regions adjacent to the insertion site were compared with the publically available genome sequence of *C. reinhardtii* (Joint Genome Institute). PCR reactions with random primers in combination with three plasmid primers revealed that the insertion of a plasmid fragment (2.4 kb) caused deletion of a 4.2 kb fragment in chromosome 11 of the *tla4* mutant (Fig. 4B). The insertion disrupted Cre11.g479750, a gene encoding the CrCpSRP54 protein and, further, Cre11.g479800, a gene of unknown function was deleted.

3.6. Complementation of the tla4 mutant

To test for a possible cause-and-effect relationship between the Cre11.g479750 or Cre11.g479800 gene deletion and the *tla4* phenotype, we performed complementation of the *tla4* mutant with each of the putative genes. Complementary DNAs (cDNAs) of Cre11.g479750 and Cre11.g479800 were cloned into pChlamy3 and then used separately to transform the *tla4* strain. pChlamy3 contains a hygromycin resistance gene that confers resistance to this antibiotic for strain selection.

Table 2
Growth characteristics of wild type and *tla4* mutant grown under 450 μmol photons m^{-2} s^{-1} (n = 3; values shown are means ± SD). a, b indicate significantly different results ($p < 0.001$) and c, d indicate significantly different results ($p < 0.01$) as determined by Student *t*-test.

Strain	Growth rate (μ h^{-1})	Stationary phase cell density (10^7 cells/mL)
WT	0.097 ± 0.007[a]	4.093 ± 0.051[c]
tla4	0.154 ± 0.005[b]	4.712 ± 0.116[d]

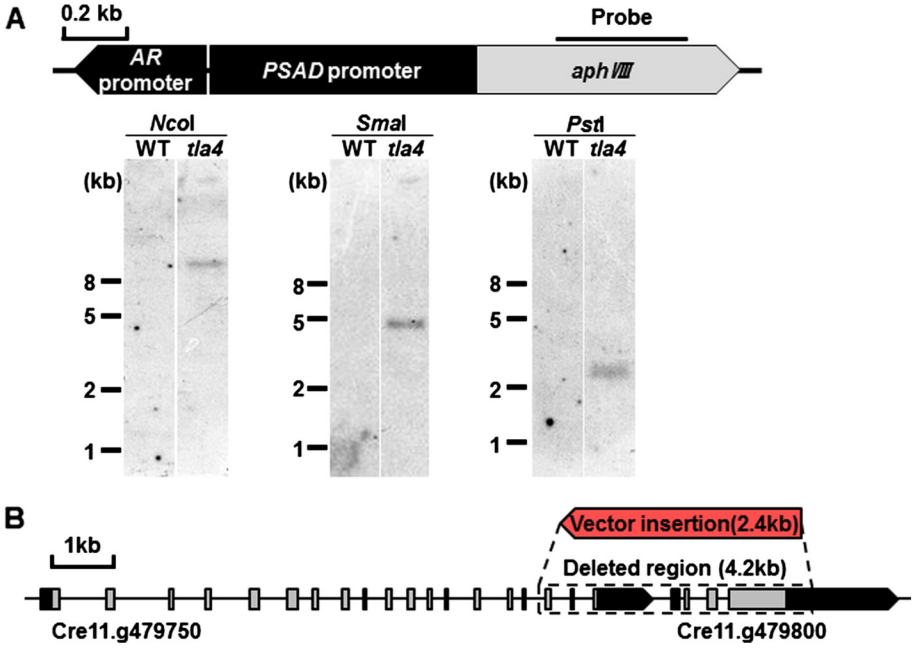

Fig. 4. Genomic DNA organization of the *tla4* mutant. A, Southern blot analysis. Genomic DNA was digested with *Nco*I, *Sma*I, or *Pst*I. A partial sequence of the *aphVIII* gene was used as a probe. B, Map of the insertion site in the genomic DNA. The areas marked with a broken line are nucleotides deleted in the *tla4* mutant, including a CpSRP54 homolog (g479750) and a portion of the g479800 gene. The red box indicates the plasmid inserted in the deleted region. Arrows indicate the direction of the insertions. Black: untranslated regions. Gray: exons. Horizontal lines: introns.

Complemented strains grown on hygromycin-containing media were screened to assess color appearance and the Chl *a*/*b* ratio. The pChlamy3-Cre11.g479750 (Fig. 5), but not pChlamy3-Cre11.g479800 construct (Supplementary Fig. S3), rescued the *tla4* phenotype. Coloration of the complemented strains with the introduced Cre11.g479750 gene cDNA was intermediate between that of the wild type and the *tla4* mutant (Fig. 5A). Complemented strains C1, C2, and C3 were selected for further characterization and analysis. The accumulation of Chl in the complemented strains was at least partially restored, and Chl content on a cell basis was slightly greater in C3 than in the wild type (Fig. 5B). The complemented strains also displayed a lower Chl *a*/*b* ratio compared to the un-complemented *tla4* mutant.

Specific polyclonal antibodies raised against a synthetic peptide of the TLA4-CrCpSRP54 protein were used in Western blot analysis to test the level of the CrCpSRP54 protein in the complemented strains. The TLA4-CrCpSRP54 protein was clearly detected in the wild-type control but not in *tla4* mutant (Fig. 5C). This cross-reaction was missing from the cell extracts of the *tla4* mutant (Fig. 5C, *tla4*), but was restored to different levels in the complemented strains (Fig. 5C, C2 and C3). It is concluded that complementation of the *tla4* mutant with the cDNA of the Cre11.g479750 gene rescued the mutation; therefore, the *tla*4 mutant phenotype was caused by a knockout of the *C. reinhardtii* homolog of the *CpSRP54* gene.

3.7. Western blot analysis of LHC proteins, reaction center, and CpSRP proteins in wild type and tla4 mutant

The smaller functional Chl antenna size of PSI and PSII in the *tla4* mutant compared to the wild type is evidence of a truncated light-harvesting antenna size in each of the photosystems. To test for changes

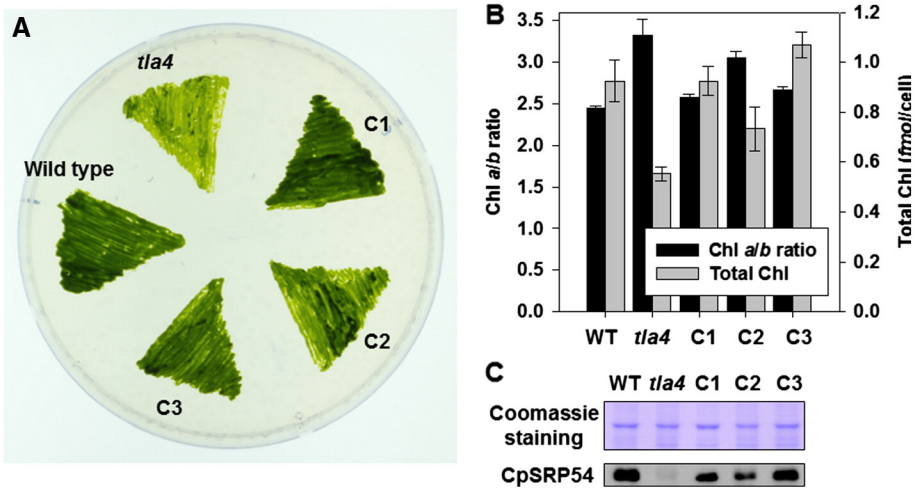

Fig. 5. A, Colonies of wild-type (WT) *C. reinhardtii* CC-4349 (parental strain of *tla4*), the *tla4* mutant, and complemented *tla4* lines (C1–C3) under photoautotrophic growth conditions. B, Chl *a*/*b* ratios of the above strains (n = 3; values shown are means ± SD). C, Western blot analysis of total protein extracts from the *C. reinhardtii* wild type (WT), the *tla4* mutant and the *tla4* complemented lines C2 and C3. Upper image shows the corresponding SDS-PAGE Coomassie–stained gel.

in the LHC protein composition of the photosystems in *tla4*, thylakoid membrane protein profiles of the wild type and the *tla4* mutant were compared. Total protein extracts of wild type and *tla4* cells were separated by SDS-PAGE and analyzed by Western blotting. To ensure linearity of the signal as a function of protein loading of the gels, protein samples of wild type were loaded at three different concentrations, and Western blots were repeated at least three times. Results of a representative experiment are shown in Figs. 6 and 7. It was observed that levels of PSII core proteins (PsbA, PsbD, and PsbO) in the *tla4* mutant samples were a bit higher than the same proteins in the wild-type samples. Levels of PSI (PsaC), the large subunit of Rubisco (RbcL) and the β-subunit of the ATP synthase (ATPβ) occurred in equivalent amounts in the wild type and *tla4* mutant (Fig. 6B). On the contrary, it is evident that LHC apoproteins occurred in lower amounts in the *tla4* than in the corresponding wild type (Fig. 7). Integration of the bands immunodetected with the various antibodies provided a relative estimate of the change in these complexes between WT and *tla4*. This qualitative analysis showed that overall LHC-I in the *tla4* mutant was lowered to about 57% of that in the wild type (Fig. 7C), whereas LHC-II in the *tla4* mutant was lowered to only about 84% of that in the wild type (Fig. 7D).

Levels of the CpSRP proteins in wild type and *tla4* mutant were also assayed by Western blot analysis with specific polyclonal antibodies. The CpFTSY and CpSRP43 proteins in the *tla4* mutant occurred at levels equivalent to those in the wild type (Fig. 8). As expected (e.g. Fig. 5) the CpSRP54 was not present in the *tla4* mutant. These results suggest that the TLA-phenotype in the *tla4* mutant can only be attributed to the absence of the *CpSRP54* gene and its encoded protein, and that no secondary/indirect effects on the abundance of the CpFTSY and CpSRP43 are involved.

3.8. The C. reinhardtii CpSRP54 protein sequence and its 3-D structure

Cre11.g479750 contains 19 exons and 18 introns. The length of the encoded mRNA is 2692 bp and the length of the coding sequence is 1650 bp. The CpSRP54 protein (549 amino acids) has a putative 63-amino-acid chloroplast-targeting sequence, as predicted by ChloroP software (http://www.cbs.dtu.dk/services/ChloroP/). According to the database of protein families (http://pfam.sanger.ac.uk), CpSRP54 consists of three domains: the SRP54 N-terminal helical bundle domain (amino acids 7–84; N domain), the SRP54-type GTPase domain (102–297; G domain), and the signal peptide–binding domain (328–426; M domain). The signal peptide–binding domain, which is universally conserved in SRP54 proteins, is also called the methionine-rich domain because it is rich in methionine residues, which contribute to signal peptide binding, as seen in cytosolic SRP54 proteins [4,33,34]. A ClustalW2.1 analysis showed that CrCpSRP54 shares 51% identity and 68% similarity with the AtCpSRP54 from *Arabidopsis thaliana*. A comparison of the amino acid sequences of the M domains of CrCpSRP54 and AtCpSRP54 revealed 47% identity and 68% similarity (Fig. 9).

Previous studies investigated the structure of the M domain of cytosolic SRP54 to understand the signal peptide binding mechanism in diverse species [4,33,34]. However, the entire 3-D structure of chloroplast SRP54 has not yet been reported. In this work, to probe for any structural difference between AtCpSRP54 and CrCpSRP54, the 3D-structures of these proteins were compared (Supplementary Fig. S5, A and B). The protein structures were predicted by the Phyre web server version 2.0 software [30]. Homology modeling of the AtCpSRP54 and CrCpSRP54 proteins, based on six templates, which include archaeal, bacterial and mammalian SRP54 proteins, was employed to maximize confidence, percentage identity and alignment coverage. 97% of residues in AtCpSRP54 modeled at ~90% confidence and 15 residues were modeled by ab initio. In the *C. reinhardtii* CpSRP54, 96% of residues modeled at ~90% confidence and 19 residues were modeled by ab initio. The sequence identity, confidence and coverage percentage between query and template sequences are shown in detail in Supplementary Table S2.

The program predicted three-dimensional structures of both CrCpSRP54 and AtCpSRP54 showed the folding of the N, G and M domains (Supplementary Fig. S5). We next looked at the CpSRP54 M-domains of the CrCpSRP54 and AtCpSRP54 in more detail. These consist of conserved α-helices (Fig. 10, A and B). Within the linear sequence of the M domains of the *C. reinhardtii* CpSRP54, compared to other land plant homologs, there are 4 α-helix motifs that define a hydrophobic rich region. However, the region between α-helix 1 and α-helix 2 also generates a finger loop displayed in predicted 3-D structures (Fig. 10). Interestingly, residues of the finger loop of CpSRP54 in *C. reinhardtii* have an extended region, occupying more space in the hydrophobic groove compared to that of *Arabidopsis* (Fig. 10B, circled). This difference between the *C. reinhardtii* and *A. thaliana* finger loops of CpSRP54 M-domains is clearly seen in the merged models (Fig. 10C, arrow). When looking in detail at the CpSRP54 M-domain extended finger loop, it was observed that an otherwise conserved Ser (hydrophilic) amino acid was missing from this domain (Fig. 9, sequence framed by a rectangle), potentially increasing the hydrophobic nature of the extended finger loop center in *C. reinhardtii*.

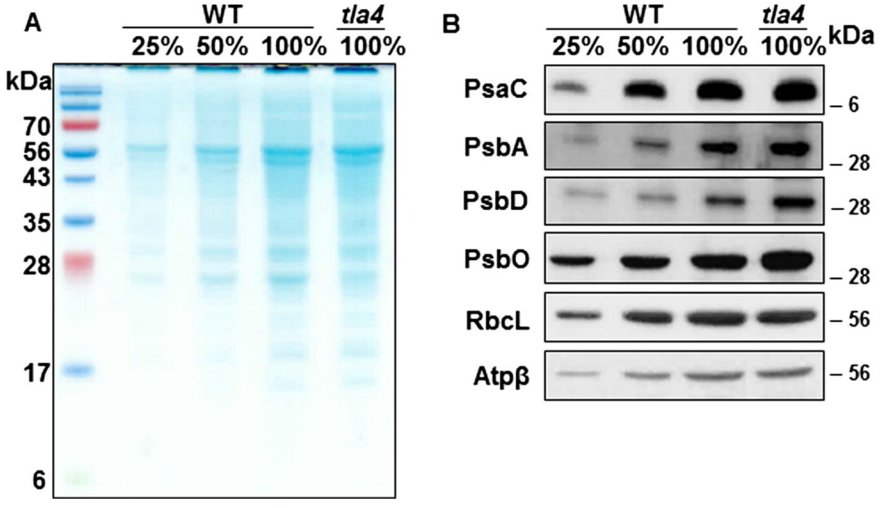

Fig. 6. SDS-PAGE of *C. reinhardtii* protein extracts and Western blot analysis of the PSI-core and PSII-core proteins in wild type (WT) and the *tla4* mutant. A, Coomassie–stained SDS-PAGE gel of protein extracts. B, Immunodetection of proteins cross-reacting with specific polyclonal antibodies against the PSI and PSII reaction center proteins (PsaC, PsaA, PsbD), a subunit of the oxygen-evolving complex (PsbO), the large subunit of Rubisco (RbcL), and the β-subunit of ATP synthase (ATPβ) of *C. reinhardtii*. The ATPβ protein was used as a loading control.

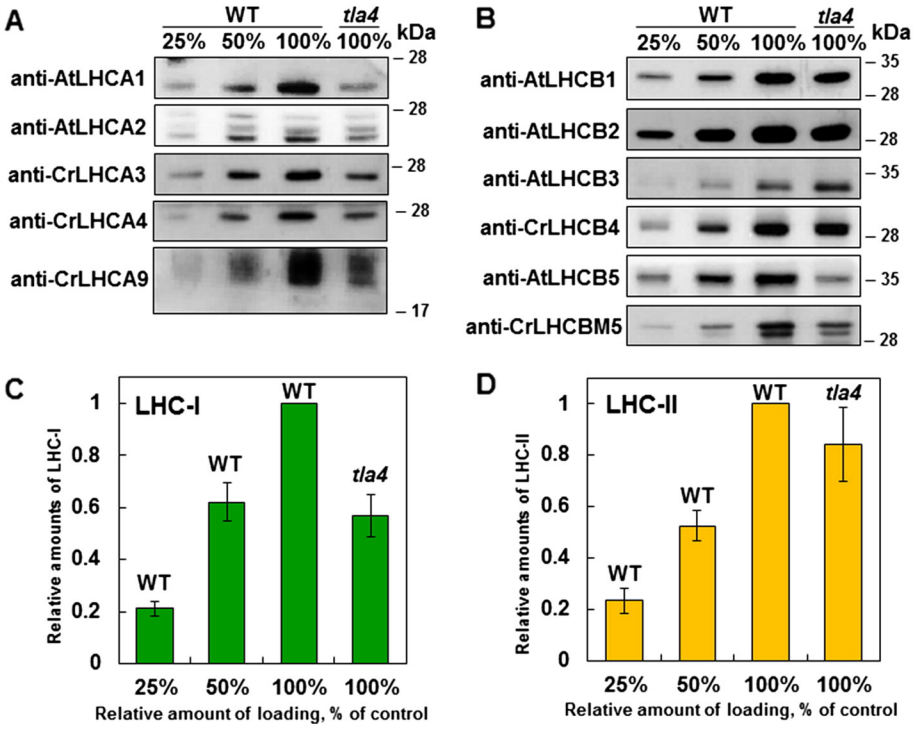

Fig. 7. Western blot analysis of the light-harvesting antenna proteins of PSII and PSI in wild type (WT) and the *tla4* mutant. Immunodetection of proteins cross-reacting with polyclonal antibodies against LHC-I and LHC-II of *Arabidopsis thaliana* and *Chlamydomonas reinhardtii* is presented in A and B, respectively. Integrated immunodetection of the LHC-I proteins based on protein bands from A is shown in C and those of LHC-II from B are shown in D, affording a measure of the change in these complexes between WT and *tla4*. Values shown are means ± SE.

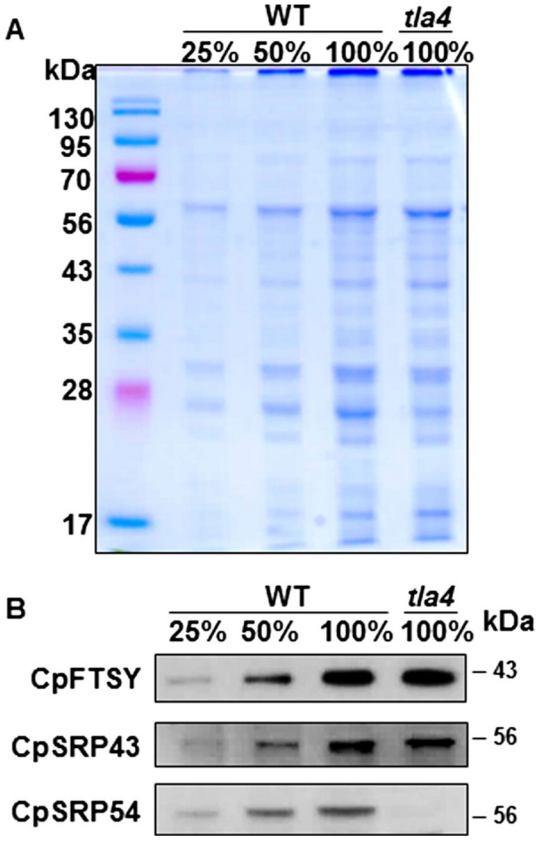

Fig. 8. SDS-PAGE of *C. reinhardtii* protein extracts and Western blot analysis of the SRP pathway proteins in wild type (WT) and the *tla4* mutant. A, Coomassie Blue–stained SDS-PAGE gel of protein extracts. B, Immunodetection of proteins cross-reacting with specific polyclonal antibodies against the CpFTSY, CpSRP43, CpSRP54 proteins of *C. reinhardtii*.

4. Discussion

The SRP pathway operates in the cytoplasm of both prokaryotes and eukaryotes. This ancient protein transport machinery mediates the co-translational transport and assembly of membrane proteins. In prokaryotes, the SRP pathway relies on the nearby presence of ribosomes and RNA components [35]. In higher plant chloroplasts, the CpSRP system handles proteins imported from the cytosol and does not interact with the mRNA polyribosome complex of the prokaryotic cells. However, the CpSRP system contains CpSRP54, an evolutionarily conserved 54-kD GTPase. The CpSRP54 participates in the co-translational targeting of chloroplast-encoded proteins to the thylakoid membrane, whereas the role of CpSRP43 is restricted to the post-translational transport of LHCPs, working in close coordination with CpFTSY and ALB3 [36,37]. *Chlamydomonas reinhardtii* possesses the CpSRP homolog pathway, which is proposed to be involved in trafficking imported light-harvesting proteins to the thylakoid membrane, thereby contributing to the biogenesis and assembly of the photosystem holocomplexes [10,11,38–40]. Previously, the *tla2* and *tla3* mutants of *C. reinhardtii* were isolated, demonstrating a drastically lower LHCP and Chl content, and a higher Chl *a*/*b* ratio than the wild type. These phenotypes were caused by the loss of function of CpFTSY (*tla2*) or CpSRP43 (*tla3*) [10,11], resulting in a substantially smaller, or truncated, light-harvesting Chl antenna size (TLA-phenotype).

In the present work, we generated truncated light-harvesting antenna size (*tla*) mutants of *C. reinhardtii* by using DNA insertional mutagenesis. One of these mutants, called *tla4*, had a truncated light-harvesting Chl antenna typical for *tla* mutants. On the basis of molecular and physiological characterizations of the *tla4* mutant and on the basis of complementation of the mutant phenotype upon transformation with a wild type copy of the CpSRP54 cDNA (Fig. 5 and Supplementary Fig. S4), we concluded that the TLA-phenotype of this mutant was associated with the loss of CpSRP54. Accordingly, the work constitutes a novel investigation and analysis of the function of the CpSRP54 in green microalgae *in vivo*.

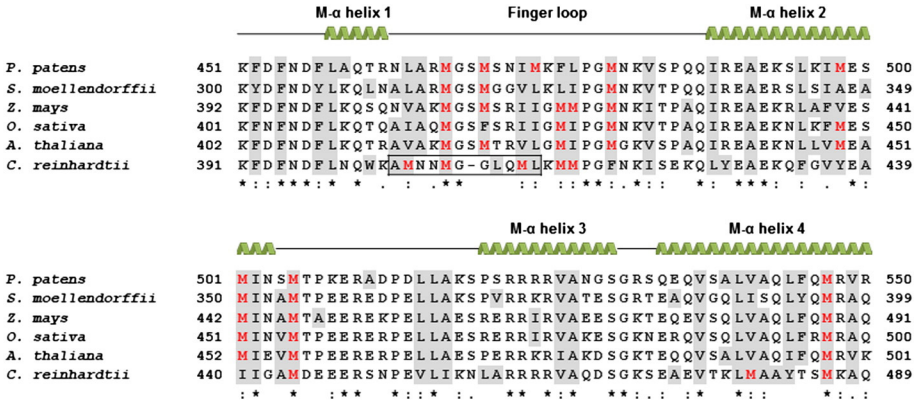

Fig. 9. Clustal W2.1 multiple sequence alignment of the M domains of *Chlamydomonas reinhardtii* CpSRP54 and homologs from *Arabidopsis thaliana* (GenBank accession no. NP_196014), *Oryza sativa* (NP_001065781), *Zea mays* (XP_008679417), *Selaginella moellendorffii* (XP_002967625), and *Physcomitrella patens* (XP_001753238). Gray boxes indicate hydrophobic residues. Methionine residues are shown in red. An asterisk indicates positions which have a single, fully conserved residue. A colon indicates conservation between groups of strongly similar properties. A period indicates conservation between groups of weakly similar properties. The residues of the extended finger loop of CpSRP54 in *C. reinhardtii* compared to that of *A. thaliana* are framed within a rectangle. The secondary structure shown above the aligned sequence was based on the predicted 3-D model of CrCpSRP54 (Fig. 10 and Supplementary Fig. S5).

The disruption of the gene encoding CpSRP54 in *C. reinhardtii* lowered the LHCP content of the cell. For example, protein bands in the *tla4* strain detected by anti-AtLHCA1 antibodies accumulated to only 25% of the wild-type level. The level of band intensities of AtLHCA2, CrLHCA3–4, CrLHCA9, AtLHCB1–2, AtLHCB5 and CrLHCBM5 in *tla4* ranged from 36% to 90% of the wild-type levels. Interestingly, protein bands detected with anti-AtLHCB3 and anti-CrLHCB4 did not seem to be substantially affected by the *tla4* mutation (Fig. 7A and B). When LHCP levels were integrated, LHCI proteins accumulated to nearly 57% of the wild-type levels (Fig. 7, A and C). The levels of LHCII proteins in *tla4* were in the range of 30% to 100%, on average, 84% of the wild-type levels (Fig. 7, B and D). The amounts of LHC proteins were consistent with the functional antenna size measurement of PSI and PSII in the *tla4* strain (Table 1). These results revealed that CpSRP54 clearly contributes to LHCP targeting and accumulation in the thylakoid membrane via the CpSRP pathway, with preference the targeting and accumulation of LHC-I. Characterization of the corresponding *Arabidopsis* mutant, *ffc*, showed that the SRP-dependent pathway is required for targeting of at least seven of the LHCPs (Lhca1, Lhca3, Lhca4, Lhcb1, Lhcb2, Lhcb3, and Lhcb5) to developing thylakoids. The amount of the seven LHCPs was lowered in the *ffc* mutant. However, elevated levels of the Lhcb4 protein, and wild type levels of Lhca2 and Lhcb6 were observed in the *ffc* mutant. These three LHCPs were either less dependent on or independent of the CpSRP assembly pathway [41], suggesting some difference between green microalgae and plants in the *in vivo* function of the CpSRP54 in terms of LHCP delivery and assembly.

The importance of the CpSRP54 for LHCP delivery has been well documented in higher plants, e.g. *Arabidopsis*. CpSRP43 binds the C-terminal tail of CpSRP54, thus forming a stable soluble heterodimer in the stroma [42,43], capable of binding and transiting hydrophobic LHCPs [40]. It was assumed that the post-translational CpSRP pathway in *C. reinhardtii* also involves CpSRP54 as a key factor (together with the CpSRP43). However, a recent *in vitro* study on the function of *C. reinhardtii* CpSRP54 concluded that it plays no role in transit complex formation with the CpSRP43, nor is it involved in LHCP recognition [44]. The implication of the latter report is that a null mutation of CpSRP54 in *C. reinhardtii* would have no or only a minor effect on LHCP delivery, which would then occur via the other components of the SRP pathway independently of the CpSRP54. In this regard, CpSRP43 would have to assume a far greater role in LHCP trafficking in green microalgae. Accordingly, the CpSRP43-null mutation in *tla3* appears to have a more severe effect on LHCP targeting than the *tla4* mutation, because the peripheral light-harvesting antenna proteins for PSII are nearly absent in the *tla3* mutant [11]. On the contrary, in the *tla4* mutant, levels of the LHC-I (Fig. 7C) appeared to have changed more that the corresponding change in the level of the LHC-II (Fig. 7D).

The *tla4* mutant, examined in this work, expresses the CpSRP43 and CpFTSY proteins to levels equivalent to those in the wild type (Fig. 8). The CpFTSY in *C. reinhardtii* (CrCpFTSY) is thought to bind the LHC-protein/CpSRP43 complex and guide it to the membrane bound translocase ALB3. This view is consistent with a recent report showing that CrCpFTSY is localized exclusively in the soluble chloroplast stroma, and this soluble CrCpFTSY specifically operates in the assembly of the peripheral components of the Chl *a-b* light-harvesting antenna [10]. Alternatively, CpSRP43 alone functions as a chaperone for LHCPs, enabling them to interact with ALB3, as seen in the corresponding CpSRP54-lacking *Arabidopsis ffc* mutant [45–47]. However, it cannot be excluded that some LHCPs are transported to the thylakoid membrane by an alternative SRP-independent pathway. Some studies have suggested that such mechanism relies on a vesicular-targeting pathway, i.e., vesicles budding from the envelope membrane and fusing with the growing thylakoids [48,49].

The role of CpSRP54 seems to be limited to primarily the assembly of the LHCA and secondarily to the assembly of some of the LHCB proteins in green microalgae. In *Arabidopsis*, CpSRP54 is required for the proper integration of other transmembrane proteins including chloroplast-

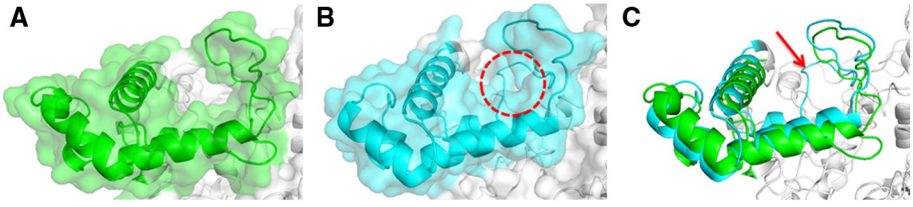

Fig. 10. Predicted tertiary folding structure of *C. reinhardtii* CpSRP54 and *A. thaliana* CpSRP54 generated by the Phyre2 program [30]. The three-dimensional structures were displayed with PyMOL v1.74 (Schrödinger, Inc.). The M domains of AtCpSRP54 (A) and CrCpSRP54 (B) are shown. A merged image of the two is shown in C. The whole protein structures of AtCpSRP54 and CrCpSRP54 were shown in Supplementary Fig. S5.

encoded protein, as evident by the phenotype caused in the corresponding knockout mutants [38,41]. In *tla4*, the CpSRP54-null mutation did not affect the integration of the psbA/D1 and psbD/D2 PSII reaction center proteins, or the psaC PSI reaction center protein, all of which occurred at the same level in *tla4* and the wild type (Fig. 6B). Hence, the CpSRP54-null mutation did not affect the assembly and integration of these PSII-core proteins in green microalgae. In contrast, in higher plants, CpSRP54 is involved in co-translational targeting of D1 to the thylakoid membrane by binding to the first transmembrane domain of the elongating nascent chain of D1 [50–52]. Additional evidence for the involvement of CpSRP54 in co-translational targeting of thylakoid membrane proteins came from the analysis of *Arabidopsis* mutants lacking functional CpSRP54 [42]. The corresponding mutant, *ffc*, showed lower levels of the D1 and D2 reaction center proteins of PSII [41,53]. The biogenesis of some chloroplast-encoded proteins that are targeted to the thylakoid membrane by the co-translational SRP pathway requires CpSRP54, possibly the chloroplast SRP receptor CpFTSY, the chloroplast SRP insertase ALB3, and the SEC translocase CpSECY [54–56].

Our results showed that CrCpSRP54 is not likely involved in the co-translational assembly pathway for the psbA/D1, psbD/D2 (PSII), and psaC (PSI) in *C. reinhardtii* (Fig. 6B). This raises a question as to how green algae target plastid-encoded proteins to the thylakoid membrane? An alternative transport-assembly pathway may be involved in the insertion of reaction center proteins in the thylakoid membrane [57–60]. It is possible that an mRNA-based mechanism targets D1 for de novo PSII assembly. The evidence for such a mechanism comes from localization of the *psbA* mRNA in specific regions of the chloroplast, referred to as translation zones, where components of the translation machinery may accumulate [61,62].

In *tla4* cells grown under medium light intensity, the total Chl content was lower by about 40% compared to that of the wild type. In the corresponding *Arabidopsis* CpSRP54-lacking *ffc* mutant, the Chl content was lowered by over 75% [41,53] with no changes in the Chl *a*/*b* ratio. In contrast, a significantly elevated Chl *a*/*b* ratio was observed in the *C. reinhardtii tla4*. The Chl *a*/*b* ratio reflects the relative abundance of LHCPs, which contain both Chl *a* and Chl *b* for their assembly and stability. Thus, the difference in pigmentation and other phenotypic differences between *tla4* and *ffc* could be explained by substantially different functional properties for the CrCpSRP54 and AtCpSRP54.

The amino acid sequence similarity between CrCpSRP54 and AtCpSRP54 is 68%, which indicates that CpSRP54 is highly conserved. However, when we compared the M domain regions of CpSRP54, the *in silico* 3-D structure modeling revealed that a part of the finger loop in CrCpSRP54 M-domain extended inward and occupied additional space in the hydrophobic groove in comparison with that of the AtCpSRP54 (Fig. 10). This distorted topology of the hydrophobic groove came about because of the extended finger loop of the CrCpSRP54 M-domain and was likely the result of a slightly different amino acid composition in this region. The finger loop motif of cytosolic SRP54 M-domain is suggested to be flexible, this feature could be important for signal recognition and sequence binding [33]. This subtle difference between the finger loops of the M domains of CrCpSRP54 and AtCpSRP54 could affect their binding capacity of hydrophobic proteins including the LHCPs, and thus lead to the phenotypic differences between *Arabidopsis thaliana* and *Chlamydomonas reinhardtii* mentioned above.

In view of the necessity to reduce carbon dioxide emissions, outlined in the 2015 Paris protocol (http://www.cop21.gouv.fr/en/), developing carbon-neutral technologies is a priority worldwide. Nature has evolved highly sophisticated mechanisms for carbon concentration, fixation, and assimilation [63]. Many novel biological carbon capture and utilization (CCU) technologies by which to convert CO_2 into fuels or value-added chemicals for human consumption could depend on the use of microalgal photosynthesis. To generate bioenergy and value-added chemicals [32,64–68], the light energy conversion efficiency of photosynthesis is thus a most critical factor for the economic viability of photosynthetic production [17]. Wild type microalgae evolved a large antenna size to be competitive and survive in the wild, where light limited conditions and competition with other plant species prevail [12]. However, under direct sunlight in commercial production cultures, when photosynthesis is saturated, wild type cells at the surface of the culture absorb excess energy that cannot be utilized but is lost to heat dissipation. This causes photodamage to the cells on the surface, whereas cells deeper in the culture are deprived of much needed sunlight for photochemistry, a condition that substantially lowers the photosynthetic efficiency and productivity of the culture [12,17,19]. In such cases, cells with a truncated antenna size will intercept fewer photons compared to the wild type at the surface of the culture, resulting in improved sunlight penetration deeper into the culture, thus affording a more uniform productivity through the depth of the culture. These features suggest truncated light-harvesting antenna (TLA) strains could afford greater productivity under bright sunlight and high cell-density conditions than wild type microalgae [12,17,19]. Actual productivity measurements in this work support these contentions (Table 2).

The *tla4* mutant exhibited a higher photosynthetic productivity (on a per Chl basis) than wild-type cells. Its smaller light-harvesting Chl antenna size required a higher light intensity to saturate photosynthesis than that required for the wild-type counterpart (Fig. 3). Furthermore, growth rate of *tla4*, as measured from the cell duplication time, was significantly greater than that of the wild type (Table 2). These results suggest that the *tla4* mutant could be more productive than the wild type under bright sunlight and high cell-density conditions. In comparison with earlier work on the *tla2* and *tla3 C. reinhardtii* mutants [10,11], which have substantially reduced levels of LHCPs (10–15% of the wild-type level) and a higher Chl *a*/*b* ratio (up to 9), the *tla*4 showed only slightly lower than wild type LHCP levels and only a moderately elevated Chl *a*/*b* ratio (<4). The level of D2 was lowered to 25% of the wild-type level in *tla2* and to 35% in *tla3*, but the D2 level in the *tla4* remained the same as in the wild type. All currently characterized TLA-type mutants in *C. reinhardtii* (ALB3.1, TLA2, TLA3, and TLA4) are capable of photoautotrophic growth. If deletion of two or all of the ALB3.1, CpFTSY, CpSRP43, and CpSRP54 genes could generate mutants with the smallest possible Chl antenna size, it would be of interest to validate the application of such mutants for carbon capture and utilization and to set the stage for further functional characterization of the CpSRP pathway in green microalgae.

Transparency document

The Transparency document associated with this article can be found, in the online version.

Acknowledgements

We thank Dr. Michael Hippler for providing specific polyclonal antibodies against LHCA 3, 4, 9 from *C. reinhardtii*. This work was supported by the Korea CCS R&D Center (KCRC) (grant number NRF-2014M1A8A1049273) funded by the Korean Government (Ministry of Science, ICT and Future Planning). This work was also supported by the Energy Efficiency & Resources Core Technology Program of the Korea Institute of Energy Technology Evaluation and Planning (KETEP), granted financial resource from the Ministry of Trade, Industry and Energy, Republic of Korea (grant number 20142020200980).

Appendix A. Supplementary data

Supplementary data to this article can be found online at http://dx.doi.org/10.1016/j.bbabio.2016.10.007.

References

[1] B.R. Green, A.H. Salter, Light regulation of nuclear-encoded thylakoid proteins, Oxford University Press, Oxford, UK, 1996 (Place Published).

[2] X. Li, R. Henry, J. Yuan, K. Cline, N.E. Hoffman, A chloroplast homologue of the signal recognition particle subunit SRP54 is involved in the posttranslational integration of a protein into thylakoid membranes, Proc. Natl. Acad. Sci. 92 (1995) 3789–3793.
[3] D. Schuenemann, S. Gupta, F. Persello-Cartieaux, V.I. Klimyuk, J.D.G. Jones, L. Nussaume, N.E. Hoffman, A novel signal recognition particle targets light-harvesting proteins to the thylakoid membranes, Proc. Natl. Acad. Sci. 95 (1998) 10312–10316.
[4] M.R. Pool, Signal recognition particles in chloroplasts, bacteria, yeast and mammals (review), Mol. Membr. Biol. 22 (2005) 3–15.
[5] T. Tzvetkova-Chevolleau, C. Hutin, L.D. Noël, R. Goforth, J.P. Carde, S. Caffarri, I. Sinning, M. Groves, J.M. Teulon, N.E. Hoffman, R. Henry, M. Havaux, L. Nussaume, Canonical signal recognition particle components can be bypassed for posttranslational protein targeting in chloroplasts, Plant Cell 19 (2007) 1635–1648.
[6] S. Jansson, E. Pichersky, R. Bassi, B.R. Green, M. Ikeuchi, A. Melis, D.J. Simpson, M. Spangfort, L.A. Staehelin, J.P. Thornber, A nomenclature for the genes encoding the chlorophyll *a*/*b*-binding proteins of higher plants, Plant Mol. Biol. Report. 10 (1992) 242–253.
[7] C. Aldridge, P. Cain, C. Robinson, Protein transport in organelles: protein transport into and across the thylakoid membrane, FEBS J. 276 (2009) 1177–1186.
[8] M. Moore, R.L. Goforth, H. Mori, R. Henry, Functional interaction of chloroplast SRP/FtsY with the ALB3 translocase in thylakoids: substrate not required, J. Cell Biol. 162 (2003) 1245–1254.
[9] F. Ossenbühl, V. Göhre, J. Meurer, A. Krieger-Liszkay, J.D. Rochaix, L.A. Eichacker, Efficient assembly of photosystem II in *Chlamydomonas reinhardtii* requires Alb3.1p, a homolog of *Arabidopsis* ALBINO3, Plant Cell 16 (2004) 1790–1800.
[10] H. Kirst, J.G. García-Cerdán, A. Zurbriggen, A. Melis, Assembly of the light-harvesting chlorophyll antenna in the green alga *Chlamydomonas reinhardtii* requires expression of the TLA2-CpFTSY gene, Plant Physiol. 158 (2012) 930–945.
[11] H. Kirst, J.G. Garcia-Cerdan, A. Zurbriggen, T. Ruehle, A. Melis, Truncated photosystem chlorophyll antenna size in the green microalga *Chlamydomonas reinhardtii* upon deletion of the TLA3-CpSRP43 gene, Plant Physiol. 160 (2012) 2251–2260.
[12] H. Kirst, A. Melis, The chloroplast signal recognition particle (CpSRP) pathway as a tool to minimize chlorophyll antenna size and maximize photosynthetic productivity, Biotechnol. Adv. 32 (2014) 66–72.
[13] Y. Nakajima, R. Ueda, Improvement of photosynthesis in dense microalgal suspension by reduction of light harvesting pigments, J. Appl. Phycol. 9 (1997) 503–510.
[14] A. Melis, J. Neidhardt, J.R. Benemann, *Dunaliella salina* (Chlorophyta) with small chlorophyll antenna sizes exhibit higher photosynthetic productivities and photon use efficiencies than normally pigmented cells, J. Appl. Phycol. 10 (1998) 515–525.
[15] J.E.W. Polle, S. Kanakagiri, E. Jin, T. Masuda, A. Melis, Truncated chlorophyll antenna size of the photosystems—a practical method to improve microalgal productivity and hydrogen production in mass culture, Int. J. Hydrog. Energy 27 (2002) 1257–1264.
[16] J.E.W. Polle, S.D. Kanakagiri, A. Melis, tla1, a DNA insertional transformant of the green alga *Chlamydomonas reinhardtii* with a truncated light-harvesting chlorophyll antenna size, Planta 217 (2003) 49–59.
[17] A. Melis, Solar energy conversion efficiencies in photosynthesis: minimizing the chlorophyll antennae to maximize efficiency, Plant Sci. 177 (2009) 272–280.
[18] M. Mitra, A. Melis, Optical properties of microalgae for enhanced biofuels production, Opt. Express 16 (2008) 21807–21820.
[19] D.R. Ort, X. Zhu, A. Melis, Optimizing antenna size to maximize photosynthetic efficiency, Plant Physiol. 155 (2011) 79–85.
[20] E. Harris, *Chlamydomonas* Handbook, Academic Press, Inc., New York, 1989 Place Published.
[21] K.L. Kindle, High-frequency nuclear transformation of *Chlamydomonas reinhardtii*, Proc. Natl. Acad. Sci. 87 (1990) 1228–1232.
[22] H. Takahashi, S. Schmollinger, J.H. Lee, M. Schroda, F. Rappaport, F.A. Wollman, O. Vallon, The PETO protein interacts with other effectors of cyclic electron flow in *Chlamydomonas*, Molecular Plant 9 (2016) 558–568.
[23] M. Holden, Chlorophylls, Trevor Walworth Goodwin, 1976 (Place Published).
[24] H.K. Lichtenthaler, Chlorophyll and carotenoids: pigments of photosynthetic biomembranes, Methods Enzymol. 148 (1987) 350–382.
[25] A. Melis, J.S. Brown, Stoichiometry of system I and system II reaction centers and of plastoquinone in different photosynthetic membranes, Proc. Natl. Acad. Sci. 77 (1980) 4712–4716.
[26] A. Melis, Spectroscopic methods in photosynthesis: photosystem stoichiometry and chlorophyll antenna size, Philos. Trans. R. Soc. Lond. B: Biol. Sci. 323 (1989) 397–409.
[27] M. Levasseur, P.A. Thompson, P.J. Harrison, Physiological acclimation of marine phytoplankton to different nitrogen sources, J. Phycol. 29 (1993) 587–595.
[28] U.K. Laemmli, Cleavage of structural proteins during the assembly of the head of bacteriophage T4, Nature 227 (1970) 680–685.
[29] D. Petroutsos, A. Busch, I. Janßen, K. Trompelt, S.V. Bergner, S. Weinl, M. Holtkamp, U. Karst, J. Kudla, M. Hippler, The chloroplast calcium sensor CAS is required for photoacclimation in *Chlamydomonas reinhardtii*, Plant Cell 23 (2011) 2950–2963.
[30] L.A. Kelley, S. Mezulis, C.M. Yates, M.N. Wass, M.J.E. Sternberg, The Phyre2 web portal for protein modeling, prediction and analysis, Nat. Protoc. 10 (2015) 845–858.
[31] B.A. Greene, L.A. Staehelin, A. Melis, Compensatory alterations in the photochemical apparatus of a photoregulatory, chlorophyll *b*-deficient mutant of maize, Plant Physiol. 87 (1988) 365–370.
[32] S.D. Tetali, M. Mitra, A. Melis, Development of the light-harvesting chlorophyll antenna in the green alga *Chlamydomonas reinhardtii* is regulated by the novel Tla1 gene, Planta 225 (2006) 813–829.
[33] R.J. Keenan, D.M. Freymann, P. Walter, R.M. Stroud, Crystal structure of the signal sequence binding subunit of the signal recognition particle, Cell 94 (1998) 181–191.
[34] C.Y. Janda, J. Li, C. Oubridge, H. Hernandez, C.V. Robinson, K. Nagai, Recognition of a signal peptide by the signal recognition particle, Nature 465 (2010) 507–510.
[35] J. Luirink, I. Sinning, SRP-mediated protein targeting: structure and function revisited, Biochim. Biophys. Acta, Mol. Cell Res. 1694 (2004) 17–35.
[36] D. Schünemann, Mechanisms of protein import into thylakoids of chloroplasts, Biol. Chem. 388 (2007) 907–915.
[37] C.V. Richter, T. Bals, D. Schünemann, Component interactions, regulation and mechanisms of chloroplast signal recognition particle-dependent protein transport, Eur. J. Cell Biol. 89 (2010) 965–973.
[38] S. Bellafiore, P. Ferris, H. Naver, V. Göhre, J.D. Rochaix, Loss of Albino3 leads to the specific depletion of the light-harvesting system, Plant Cell 14 (2002) 2303–2314.
[39] V. Göhre, F. Ossenbühl, M. Crèvecoeur, L.A. Eichacker, J.D. Rochaix, One of two Alb3 proteins is essential for the assembly of the photosystems and for cell survival in *Chlamydomonas*, Plant Cell 18 (2006) 1454–1466.
[40] C. Träger, M.A. Rosenblad, D. Ziehe, C. Garcia-Petit, L. Schrader, K. Kock, C. Vera Richter, B. Klinkert, F. Narberhaus, C. Herrmann, E. Hofmann, H. Aronsson, D. Schünemann, Evolution from the prokaryotic to the higher plant chloroplast signal recognition particle: the signal recognition particle RNA is conserved in plastids of a wide range of photosynthetic organisms, Plant Cell 24 (2012) 4819–4836.
[41] P. Amin, D.A.C. Sy, M.L. Pilgrim, D.H. Parry, L. Nussaume, N.E. Hoffman, *Arabidopsis* mutants lacking the 43- and 54-kilodalton subunits of the chloroplast signal recognition particle have distinct phenotypes, Plant Physiol. 121 (1999) 61–70.
[42] S. Funke, T. Knechten, J. Ollesch, D. Schünemann, A unique sequence motif in the 54-kDa subunit of the chloroplast signal recognition particle mediates binding to the 43-kDa subunit, J. Biol. Chem. 280 (2005) 8912–8917.
[43] I. Holdermann, N.H. Meyer, A. Round, K. Wild, M. Sattler, I. Sinning, Chromodomains read the arginine code of post-translational targeting, Nat. Struct. Mol. Biol. 19 (2012) 260–263.
[44] B. Dünschede, C. Träger, C.V. Schröder, D. Ziehe, B. Walter, S. Funke, E. Hofmann, D. Schünemann, Chloroplast SRP54 was recruited for posttranslational protein transport via complex formation with chloroplast SRP43 during land plant evolution, J. Biol. Chem. 290 (2015) 13104–13114.
[45] T. Bals, B. Dünschede, S. Funke, D. Schünemann, Interplay between the cpSRP pathway components, the substrate LHCP and the translocase Alb3: an *in vivo* and *in vitro* study, FEBS Lett. 584 (2010) 4138–4144.
[46] S. Falk, I. Sinning, The C terminus of Alb3 interacts with the chromodomains 2 and 3 of cpSRP43, J. Biol. Chem. 285 (2010) le25–le26.
[47] N.E. Lewis, A.D. Kight, A. Daily, T.K.S. Kumar, R.L. Henry, R.L. Goforth, Response to Falk and Sinning: the C terminus of Alb3 interacts with the chromodomains 2 and 3 of cpSRP43, J. Biol. Chem. 285 (2010) le26–le28.
[48] U.C. Vothknecht, P. Westhoff, Biogenesis and origin of thylakoid membranes, Biochim. Biophys. Acta, Mol. Cell Res. 1541 (2001) 91–101.
[49] J. Kenneth Hoober, L.L. Eggink, Assembly of light-harvesting complex II and biogenesis of thylakoid membranes in chloroplasts, Photosynth. Res. 61 (1999) 197–215.
[50] R. Nilsson, J. Brunner, N.E. Hoffman, K.J. van Wijk, Interactions of ribosome nascent chain complexes of the chloroplast-encoded D1 thylakoid membrane protein with cpSRP54, EMBO J. 18 (1999) 733–742.
[51] R. Nilsson, K.J. van Wijk, Transient interaction of cpSRP54 with elongating nascent chains of the chloroplast-encoded D1 protein; 'cpSRP54 caught in the act', FEBS Lett. 524 (2002) 127–133.
[52] L. Zhang, E.M. Aro, Synthesis, membrane insertion and assembly of the chloroplast-encoded D1 protein into photosystem II, FEBS Lett. 512 (2002) 13–18.
[53] M.L. Pilgrim, K.J. van Wijk, D.H. Parry, D.A.C. Sy, N.E. Hoffman, Expression of a dominant negative form of cpSRP54 inhibits chloroplast biogenesis in *Arabidopsis*, Plant J. 13 (1998) 177–186.
[54] L. Zhang, V. Paakkarinen, M. Suorsa, E.M. Aro, A SecY homologue is involved in chloroplast-encoded D1 protein biogenesis, J. Biol. Chem. 276 (2001) 37809–37814.
[55] E. Klostermann, I. Droste gen Helling, J.P. Carde, D. SchÜNemann, The thylakoid membrane protein ALB3 associates with the cpSecY-translocase in *Arabidopsis thaliana*, Biochem. J. 368 (2002) 777–781.
[56] J.C. Pasch, J. Nickelsen, D. Schünemann, The yeast split-ubiquitin system to study chloroplast membrane protein interactions, Appl. Microbiol. Biotechnol. 69 (2005) 440–447.
[57] L.A. Eichacker, R. Henry, Function of a chloroplast SRP in thylakoid protein export, Biochim. Biophys. Acta, Mol. Cell Res. 1541 (2001) 120–134.
[58] H. Mori, K. Cline, Post-translational protein translocation into thylakoids by the Sec and ΔpH-dependent pathways, Biochim. Biophys. Acta, Mol. Cell Res. 1541 (2001) 80–90.
[59] C. Robinson, A. Bolhuis, Protein targeting by the twin-arginine translocation pathway, Nat. Rev. Mol. Cell Biol. 2 (2001) 350–356.
[60] A. Stengel, J. Soll, B. Bölter, Protein import into chloroplasts: new aspects of a well-known topic, Biol. Chem. 388 (2007) 765–772.
[61] J. Uniacke, W. Zerges, Photosystem II assembly and repair are differentially localized in *Chlamydomonas*, Plant Cell 19 (2007) 3640–3654.
[62] J. Uniacke, W. Zerges, Chloroplast protein targeting involves localized translation in *Chlamydomonas*, Proc. Natl. Acad. Sci. 106 (2009) 1439–1444.
[63] P. Jajesniak, H.E.M.O. Ali, T.S. Wong, Carbon dioxide capture and utilization using biological systems: opportunities and challenges, J. Bioprocess. Biotech. 4 (2014) 155.
[64] S.P. Mayfield, A.L. Manuell, S. Chen, J. Wu, M. Tran, D. Siefker, M. Muto, J. Marin-Navarro, *Chlamydomonas reinhardtii* chloroplasts as protein factories, Curr. Opin. Biotechnol. 18 (2007) 126–133.
[65] J.H. Mussgnug, S. Thomas-Hall, J. Rupprecht, A. Foo, V. Klassen, A. McDowall, P.M. Schenk, O. Kruse, B. Hankamer, Engineering photosynthetic light capture: impacts on improved solar energy to biomass conversion, Plant Biotechnol. J. 5 (2007) 802–814.
[66] Q. Hu, M. Sommerfeld, E. Jarvis, M. Ghirardi, M. Posewitz, M. Seibert, A. Darzins, Microalgal triacylglycerols as feedstocks for biofuel production: perspectives and advances, Plant J. 54 (2008) 621–639.
[67] H.C. Greenwell, L.M.L. Laurens, R.J. Shields, R.W. Lovitt, K.J. Flynn, Placing microalgae on the biofuels priority list: a review of the technological challenges, J. R. Soc. Interface 7 (2010) 703–726.
[68] T.M. Mata, A.A. Martins, N.S. Caetano, Microalgae for biodiesel production and other applications: a review, Renew. Sust. Energ. Rev. 14 (2010) 217–232.